

Phase transitions in nanoparticles of BaTiO₃ as functions of temperature and pressure

Wei Han, Jinlong Zhu, Sijia Zhang, Hui Zhang, Xiaohui Wang et al.

Citation: *J. Appl. Phys.* **113**, 193513 (2013); doi: 10.1063/1.4806996

View online: <http://dx.doi.org/10.1063/1.4806996>

View Table of Contents: <http://jap.aip.org/resource/1/JAPIAU/v113/i19>

Published by the [American Institute of Physics](#).

Additional information on J. Appl. Phys.

Journal Homepage: <http://jap.aip.org/>

Journal Information: http://jap.aip.org/about/about_the_journal

Top downloads: http://jap.aip.org/features/most_downloaded

Information for Authors: <http://jap.aip.org/authors>

ADVERTISEMENT

The advertisement banner for AIP Advances features a light green background with a pattern of thin, curved, wavy lines in a darker green shade. On the left, the text 'AIPAdvances' is displayed in a green, sans-serif font, with a series of orange dots of varying sizes arranged in a curved path above the word 'Advances'. On the right, there is a circular seal with a green border and a white center, containing the text 'Now Indexed in Thomson Reuters Databases'. Below the main text, there is a dark blue horizontal bar with the text 'Explore AIP's open access journal:' in white. To the right of this bar, there is a list of three bullet points in white text: '• Rapid publication', '• Article-level metrics', and '• Post-publication rating and commenting'.

AIPAdvances

Now Indexed in
Thomson Reuters
Databases

Explore AIP's open access journal:

- Rapid publication
- Article-level metrics
- Post-publication rating and commenting

Phase transitions in nanoparticles of BaTiO₃ as functions of temperature and pressure

Wei Han,¹ Jinlong Zhu,^{1,a)} Sijia Zhang,¹ Hui Zhang,² Xiaohui Wang,² Qinglin Wang,³ Chunxiao Gao,³ and Changqing Jin¹

¹National Lab for Condensed Matter Physics, Institute of Physics, Chinese Academy of Sciences, Beijing 100190, China

²Department of Material Science and Engineering, State Key Lab of New Ceramic and Fine Processing, Tsinghua University, Beijing 100084, China

³State Key Laboratory for Superhard Materials, Institute of Atomic and Molecular Physics, Jilin University, Changchun 130012, China

(Received 26 March 2013; accepted 30 April 2013; published online 21 May 2013)

We studied the temperature and pressure structural stability of 5 nm BaTiO₃ particles by using high resolution synchrotron X-ray diffraction, high pressure Raman spectroscopy, and high pressure impedance technique. A coexistence of the tetragonal and orthorhombic phases is observed in 5 nm Barium titanate BaTiO₃ particles with weight fractions 67(6.6)% and 33(8.0)% at ambient condition, respectively. In the temperature range from -123°C to 177°C , the phase boundaries of 5 nm BaTiO₃ are diffusive and several phases coexist. Pressure dependent Raman spectra of 5 nm BaTiO₃ indicates that there exist two phase transitions: the first is at 7.5 GPa when the coexisting phases of orthorhombic and tetragonal undergoes transition to tetragonal phase; the second is around 17.3 GPa when the tetragonal transforms to cubic phase. Observed transitions were confirmed by the high pressure impedance property measurement. © 2013 AIP Publishing LLC. [<http://dx.doi.org/10.1063/1.4806996>]

I. INTRODUCTION

Barium titanate BaTiO₃ (BTO) is a well known perovskite-type ferroelectric compound, which is widely used in the electronic industry.¹ At ambient pressure with decreasing temperature, BTO undergoes several structural phase transitions from cubic ($Pm-3m$) (C) to tetragonal ($P4mm$) (T) at 130°C and then to orthorhombic ($Amm2$) (O) and rhombohedral ($R3m$) (R) at 5°C and at -90°C , respectively.² The high temperature C phase is paraelectric, and the other three phases are all ferroelectrics. Previously reported studies on BTO under high pressure, using a diamond anvil cell (DAC) include dielectric measurements,^{3,4} Brillouin scattering,^{5,6} Raman scattering,⁷⁻⁹ X-ray diffraction,¹⁰ and a pulsed photoacoustic technique.¹¹ From these studies, it has been established that properties of BTO, such as the dielectric constants, the transition temperature, and the spontaneous polarization, have a tendency to decrease with increasing pressure in certain pressure region. Both single-crystal and polycrystalline BTO samples undergo a transition from the ferroelectric T phase to the paraelectric C phase at approximately 2.3 GPa at room temperature.^{8,9,12,13} Furthermore, like other perovskite-type ferroelectrics, such as isostructural KNbO₃ and PbTiO₃,^{14,15} the phase transition induced by pressure provides a representative example for studying the ferroelectric-to-paraelectric transition, which will provide an effective way to understand the driving force of perovskite-type ferroelectrics under pressure.

The crystal structure and the dielectric property of BTO depend on various factors, such as size and stress. For instance, coexistence of O and T phases was reported for the 8 nm BTO at room temperature, which can hold up to 400°C , then transforms to a C phase.¹⁶ The stress distribution on the surface of nano BTO particles can significantly change the phase boundary.^{17,18} Although number of experimental investigation on the size effects of coarse size BTO as functions of temperature and pressure have been carried out, there is very little work on phase transitions of nano BTO particles as functions of temperature and pressure. In this work, we report the study of the high resolution synchrotron diffraction of 5 nm BTO particles as a function of temperature, the Raman spectroscopy and impedance measurement of 5 nm BTO particles under high pressure. Our results indicate that a coexistence of the T and O phases is observed in 5 nm BTO particles with weight fractions 67(6.6)% and 33(8.0)% at ambient condition. The 5 nm BTO is mainly phase coexisting in the temperature range from -123°C to 177°C . 5 nm BTO keeps its ferroelectricity in a wide temperature range. High pressure *in situ* Raman spectra show evidence for two structural phase transition of 5 nm BTO particles: one is at about 7.5 GPa, which corresponds to the transition to T phase from the coexistence of O and T phases; the other is around 17.3 GPa, the T phase transformed to C phase, which is further confirmed by the anomaly located at around 18 GPa of the high pressure impedance property measurement.

II. EXPERIMENTAL

The 5 nm BTO particles were produced by chemical method described elsewhere.¹⁹ The 5 nm BTO particles in

^{a)}Author to whom correspondence should be addressed. Electronic mail: jlzhu04@iphy.ac.cn

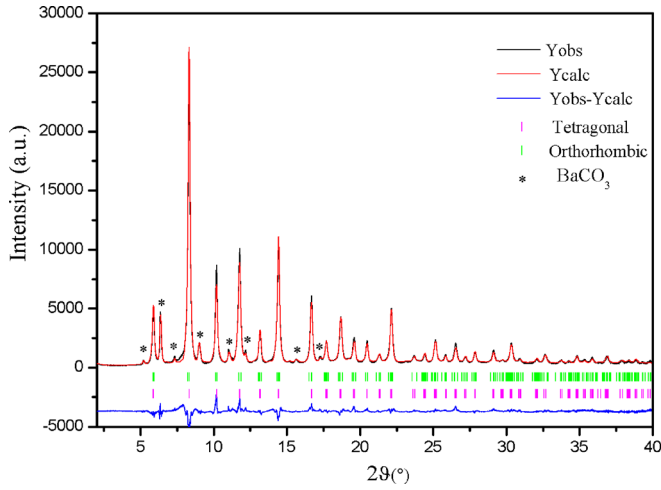


FIG. 1. High resolution X-ray diffraction pattern of nano BaTiO₃ with particle size 5 nm.

Ref. 19 show an average size of 5 nm with a narrow size distribution and a lattice tetragonality of 1.007(1). High resolution synchrotron angle diffraction with a wavelength 0.4124 Å were performed at APS, 11-BM-B, Argonne National Laboratory. High pressure Raman experiment was carried out using a Mao-Bell type DAC, with a T301 steel gasket prepressed to around 40 μm in thickness and 200 μm holes drilled serving as the sample chamber. 4:1 methanol-ethanol mixture and a 5 μm ball shape ruby were loaded together with the sample, serving as a hydrostatic pressure medium and pressure calibration by the standard ruby fluorescence method. Raman spectra were collected in backscattering geometry at room temperature by a Jobin Yvon HR800 triple spectrometer equipped with a cooled charge-couple device. In the spectrometer, a long focus objective of 20× magnification was used to focus the laser beam on the sample surface and to collect the scattered light. Raman spectra were excited with 532.0 nm radiation from a coherent solid-state laser. The laser power at the focus spot of about 1 μm in diameter was kept about 4.8 mW to obtain high quality spectra and prevent laser-induced damage to the samples. *In situ* impedance measurements in DAC under high pressure were done in Jilin University described elsewhere.²⁰

III. RESULTS AND DISCUSSION

Raman and the XRD results indicate coexisting phases at ambient condition for 5 nm BTO.¹⁹ To confirm this phase coexistence, we employed the Rietveld refinement by using the GSAS software package²¹ to identify the crystal structure of 5 nm BTO. Fig. 1 shows the structural refinement pattern of BTO using high resolution synchrotron X-ray diffraction data. The refinement smoothly converged to $R_p = 5.90\%$ and $R_{wp} = 6.97\%$, respectively. The refinement indicates that the best fitting of the diffraction pattern is a coexistence of T and O phases with the mass fractions 67(6.6)% and 33(8.0)%, respectively. The line broadening effect is caused by the fine grains, and the grain size can be estimated as 4.7 nm by using Scherrer's equation. Lattice parameters for tetragonal phase are $a = b = 4.010(7)$ Å, $c = 4.031(3)$ Å, and for orthorhombic phase are $a = 3.988(4)$ Å, $b = 5.686(3)$ Å, $c = 5.744(2)$ Å. Table I gives the structural parameters obtained from the Rietveld refinement. Fig. 2, which was reprinted from our previous work,²² gives the phase fractions of 5 nm BTO at different temperature from -123°C to 177°C by Rietveld refinement analysis of the high resolution synchrotron angle diffractions. Compared with single crystal and coarse size BTO, the phase boundaries of 5 nm BTO become more diffusive. The R, O, and T phases all extend their existing temperature region making a wide range of coexisting phase regions. The (a) particle size distribution,¹⁹ (b) type of stresses and their distributions on the particle surface,¹⁸ and (c) bond defects on the surface of 5 nm BTO particles will finally cause phase diffusion and coexistence. However, the most important is that 5 nm BTO still hold its ferroelectricity in a wide temperature range, which satisfies the industrial application with such a small particle size.

Phase coexistence evolution as function of particles sizes and temperature was reported by Zhu *et al.*²² Their results show that phase fractions and phase transition temperature were not monotonously decreased or increased. Phase reentrance was observed at around 20 nm BTO particle. This phenomenon is not following the general prediction that the ferroelectric phase will vanish for BTO with smaller nano particles. Various BTO structures were reported by different synthesis with particle sizes around 10 nm. Monodisperse

TABLE I. Structural parameters for 5 nm BaTiO₃ obtained from the structural refinement using high resolution synchrotron X-ray diffraction data at ambient condition.

Symmetry and lattice parameters	Sites	Atomic coordinates			Uiso(Å ²)
		X	Y	Z	
O: Amm2	Ba	0	0	0	0.0227
$a = 3.988(4)$ Å	Ti	0.5	0	0.541(1)	0.0020
$b = 5.686(3)$ Å	O1	0	0	0.485(4)	0.0130
$c = 5.744(2)$ Å	O2	0.5	0.254(4)	0.231(1)	0.0280
T: P4mm	Ba	0	0	0	0.0071
$a = b = 4.010(7)$ Å	Ti	0.5	0.5	0.483(7)	0.0071
$c = 4.031(3)$ Å	O1	0.5	0.5	-0.037(4)	0.0147
$c/a = 1.0051$	O2	0.5	0	0.518(4)	0.0073
Phase fraction(%)					
	Orthorhombic				Tetragonal
	33(8.0)				67(6.6)

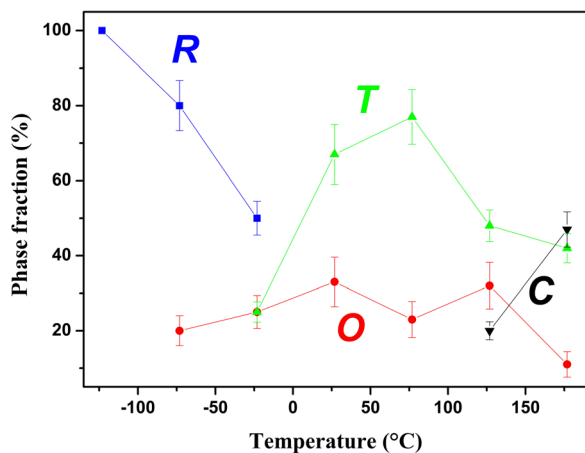


FIG. 2. Phase fraction variations of 5 nm BaTiO₃ as function of temperature from -123°C to 177°C by Rietveld analysis of the high resolution synchrotron angle diffractions. R, O, T, and C represent rhombohedral, orthorhombic, tetragonal, and cubic phases, respectively. Reprinted with permission from J. Appl. Phys. **112**, 064110 (2012). Copyright 2012 AIP Publishing LLC.

BTO particles with diameters ranging from 6 to 12 nm were indexed to cubic symmetry, which were prepared by the thermal decompositions of a metal-organic precursor.²³ The tetragonal phase BTO particles as fine as 7 nm have been synthesized using the method evolved from direct synthesis from solution.²⁴ The cubic and tetragonal modifications of the BTO perovskite structure with an average particle size of 6 nm was synthesized by the thermal decompositions of a metal-organic precursor.²⁵ The tetragonality as well as a lowered Curie transition temperature in sub-10 nm particles was established using a fungus-mediated approach.²⁶ All of ferroelectric BTO particles with sizes around 10 nm are candidates for raw material of electronic industry.

Fig. 3(a) shows the Raman spectra of 5 nm BTO with pressure up to 37.6 GPa, some peak positions are shifted, some peaks appear and some peaks disappear with increasing pressure. The main spectral features observed for 5 nm BTO are (a) intensity of the bands 184, 309, 515, and 717 cm^{-1} begins to decrease and shifts to higher frequency with increasing pressure. (b) The emerging of a shoulder near 485 cm^{-1} , which belongs to the optical phonon frequencies of T BTO, suggests that the coexisting phases of O and T transformed to T phase. (c) The T phase transforms to C phase around 17.3 GPa, which is further confirmed by the high pressure impedance property measurement. Theoretically, cubic $Pm\bar{3}m$ phase has no Raman active modes. However, the disordered character,⁸ grain boundaries, and intergrain stresses⁹ in BTO can give rise to the persistence of Raman features in cubic BTO. Furthermore, strong surface stresses and defects of the 5 nm BTO can make the Raman activations more pronounced in the cubic phase. The detailed analysis of these two phase transition will be discussed in the following paragraph. The line shape changes observed near $450\text{--}630\text{ cm}^{-1}$ between 0.3 and 37.6 GPa (see Fig. 3(a)) similar to those reported in Refs. 9, 13, and 27 which indicate some structural reordering takes place, corresponding well with discontinuities in the slopes of the phonon frequency shifts shown in Fig. 5. However, these new peaks may also be due to accumulated stresses inside the

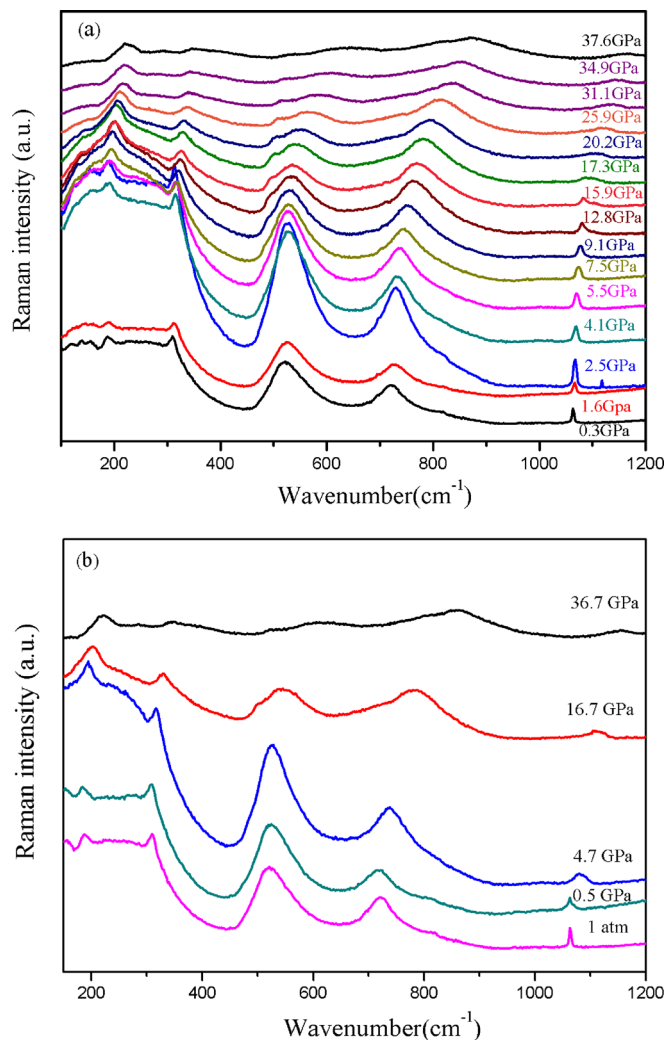


FIG. 3. Raman spectra of 5 nm BaTiO₃ in the range of $150\text{--}1200\text{ cm}^{-1}$ at different pressures (a) in the increasing pressure cycle; (b) in the decreasing pressure cycle.

sample at high pressure.^{9,13,27} Fig. 3(b) shows the Raman spectrum upon pressure release from 37.6 GPa. The broad and sharper features of the Raman spectrum are both present, and the phase transition is reversible. The result agrees well with those in Refs. 8 and 9.

The two phase transitions are verified by fitting a sum of several Lorentzian-peaks and a baseline to the normalized Raman spectra at four representative pressures: 0.3 GPa, 7.5 GPa, 17.3 GPa, and 20.2 GPa. Two peaks (located at 515 cm^{-1} and 552 cm^{-1} at 0.3 GPa) and a baseline to the normalized Raman spectra are fitted with pressure lower than 7.5 GPa, as shown in Fig. 4(a). 515 cm^{-1} belongs to coexisting phases of O and T in line with the result of synchrotron X-ray diffraction data. 552 cm^{-1} originates from some disorder of the structure which is similar to those reported in Refs. 9, 13, and 27. Three peaks, which locate at 485 cm^{-1} , 522 cm^{-1} , and 560 cm^{-1} at 7.5 GPa, and a baseline to the normalized Raman spectra are fitted between 7.5 and 17.3 GPa, as shown in Figs. 4(b) and 4(c). The emerging of a shoulder near 485 cm^{-1} , which belongs to the optical phonon frequencies of T BTO, suggests that the coexisting phases of O and T transforms to T phase. The peak located at 515 cm^{-1} shifts to 522 cm^{-1} with

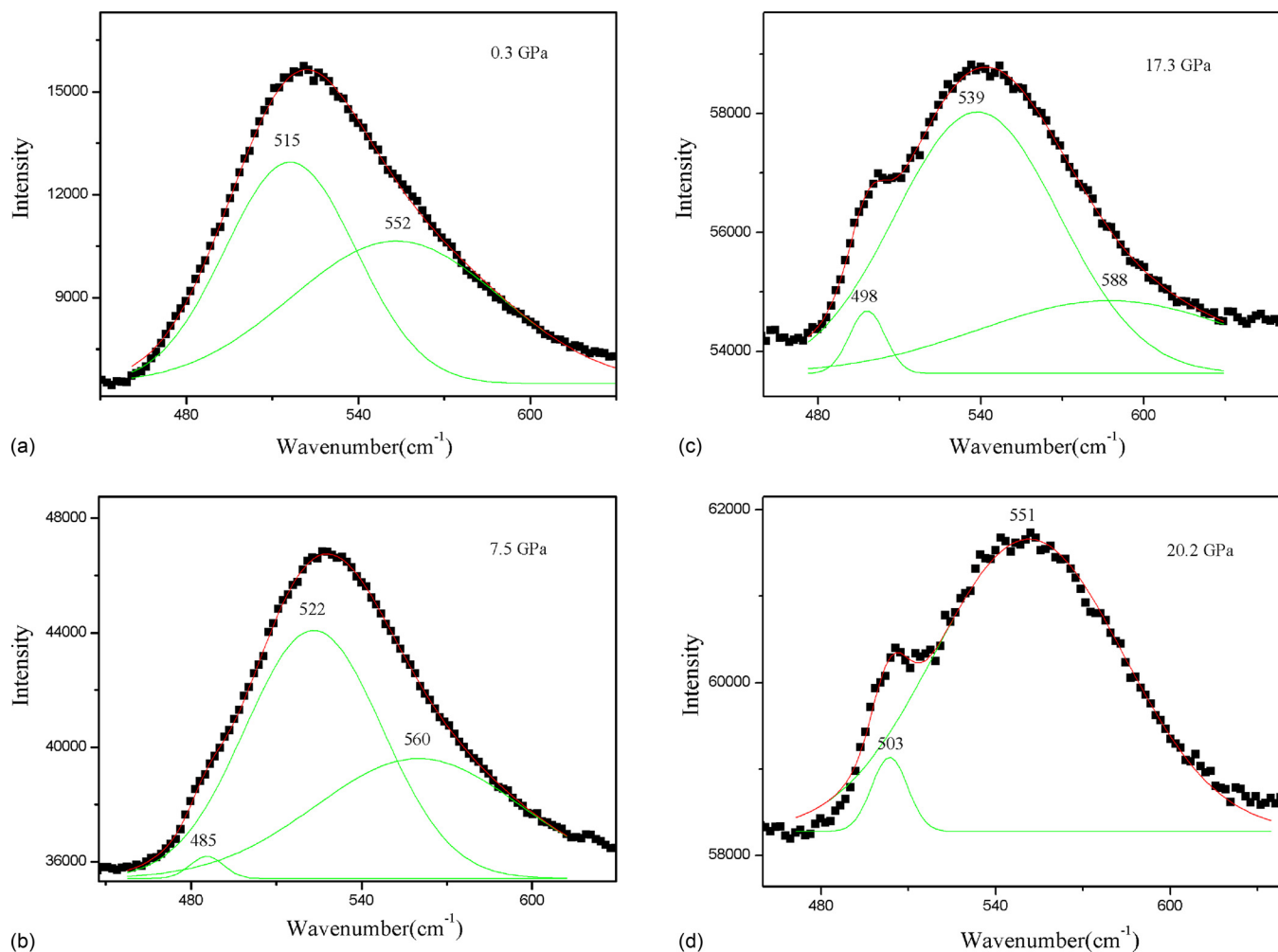


FIG. 4. Raman spectra of 5 nm BaTiO₃ in the range of 450–630 cm⁻¹ at different pressures. (a) 0.3 GPa, (b) 7.5 GPa, (c) 17.3 GPa, and (d) 20.2 GPa.

pressure increasing from 0.3 GPa to 7.5 GPa, while the peak located at 552 cm⁻¹ shifts to 560 cm⁻¹. Two peaks (located at 503 cm⁻¹ and 551 cm⁻¹ at 20.2 GPa) and a baseline to the normalized Raman spectra is fitted with pressure higher than 17.3 GPa (as shown in Fig. 4(d)). The peak located at 485 cm⁻¹ shifts to 503 cm⁻¹ with pressure increasing from 7.5 GPa to 20.2 GPa, while the peak located at 522 cm⁻¹ shifts to 551 cm⁻¹. The fitted result implies that T phase undergoes another structural reordering around 17.3 GPa. We speculate that T phase transform to C phase from the disappearance of 588 cm⁻¹ peak (at 17.3 GPa) which associates with some disorder of the structure.

The frequency positions of all the observed Raman peaks are plotted as function of pressure in Fig. 5. The frequency of the 184 cm⁻¹ increases at a rate of 1.40 cm⁻¹/GPa in the pressure range of 0–7.5 GPa, increases by 0.70 cm⁻¹/GPa between 7.5 and 17.3 GPa, and then increases at a rate of 0.93 cm⁻¹/GPa between 17.3 and 37.6 GPa. The frequency of the 485 cm⁻¹ increases at a rate of 2.96 cm⁻¹/GPa in the pressure range of 7.5–17.3 GPa, and then increases at a rate of 1.67 cm⁻¹/GPa between 17.3 and 37.6 GPa. The frequency of the 702 cm⁻¹ increases at a rate of 2.96 cm⁻¹/GPa in the pressure range of 7.5–17.3 GPa, and then increases at a rate of 4.50 cm⁻¹/GPa between 17.3 and 37.6 GPa. Both 485 cm⁻¹ and 702 cm⁻¹ have obvious changes at around

17.3 GPa indicating a phase transition. Thus, we conclude that a phase transformation from T phase to C phase occurred at around 17.3 GPa. The mode at 306 cm⁻¹ at 1 bar does not show any significant pressure-induced frequency shift anomaly in the pressure range we studied.

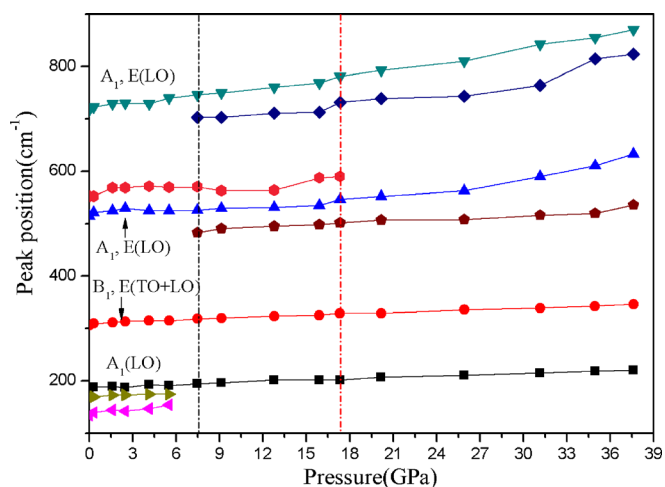


FIG. 5. Frequency of the Raman peaks observed in 5 nm BaTiO₃ plotted as a function of pressure.

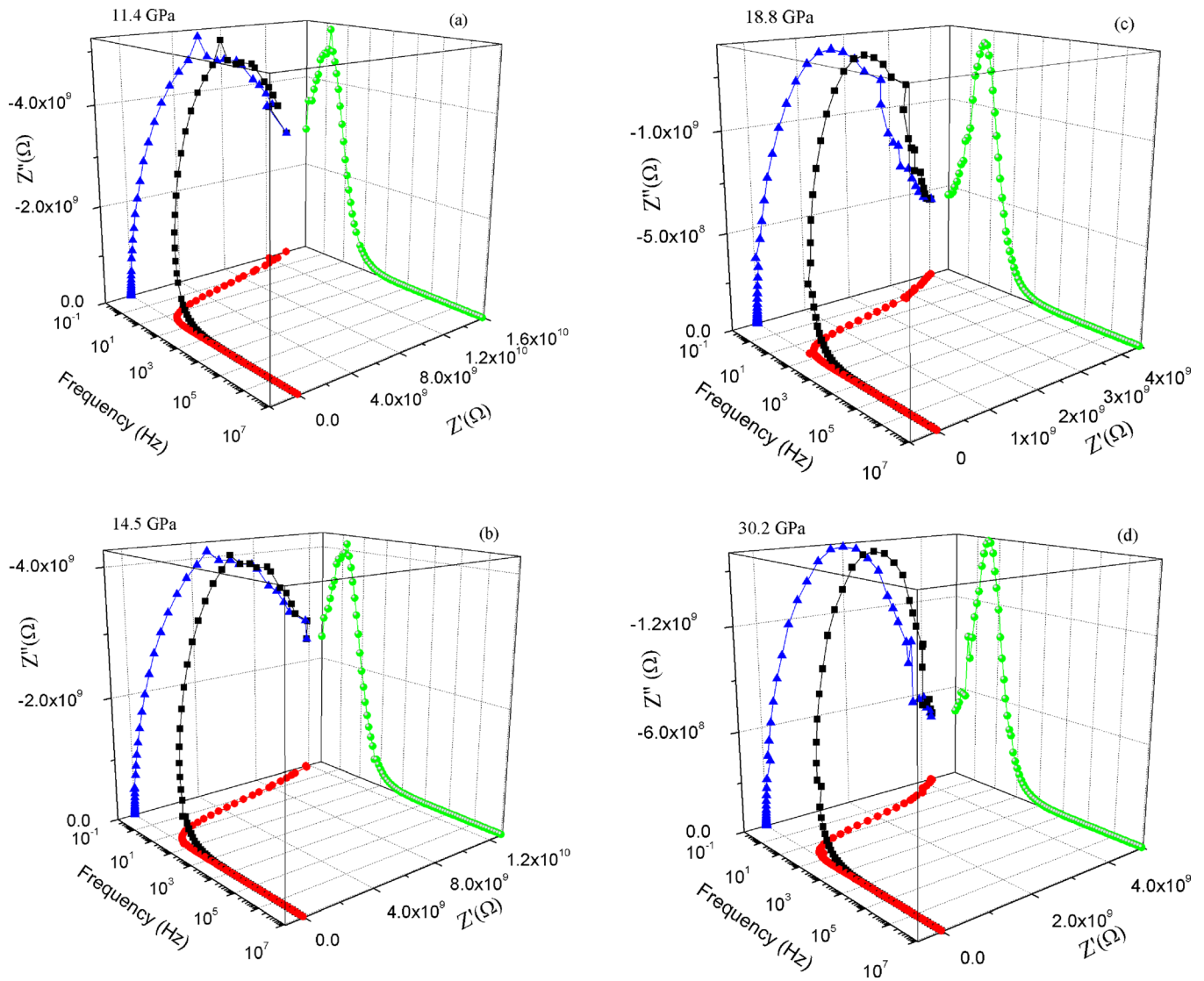


FIG. 6. Impedance of 5 nm BaTiO₃ under different pressure. (a) 11.4 GPa, (b) 14.5 GPa, (c) 18.8 GPa, and (d) 30.2 GPa.

In order to verify whether a phase transition appears or just stresses accumulating in the sample, a room temperature impedance measurement of 5 nm BTO at different pressure were carried out. Fig. 6 shows the impedance under different pressure. Impedance is represented as a complex quantity Z^* ($Z^* = Z' + i Z''$) (black plot as shown in Fig. 6), where the real part of impedance is the resistance Z' (red plot as shown in Fig. 6) and the imaginary part is the reactance Z'' (green plot as shown in Fig. 6). As shown in Fig. 6, the impedance spectrum shows an oblate-like arc closed to real axis, and the size of the arc decreases with pressure increasing. The impedance spectrum (blue plot as shown in Fig. 6) changes from open-type to closed-type indicated a structure phase transition taking place. Both the real and imaginary parts of the impedance decreased with the pressure, implying the decay of the grain boundary contribution to the electrical transmission in 5 nm BTO sample.

Fig. 7 shows the relative permittivity of sample with pressure up to 30 GPa derived from the impedance measurement. The data points below 10 GPa cannot be obtained due to the extremely large resistance, which may arise from the

loose connection between the wires and sample. There is an impedance anomaly around 18 GPa, which indicates that a phase transition occurs. This phase transition has not been

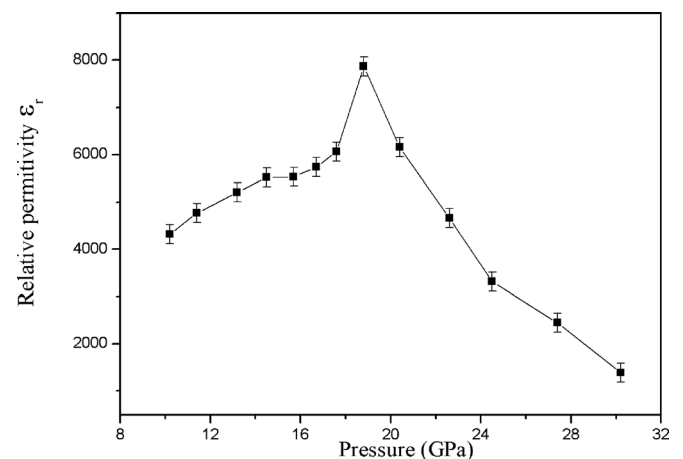


FIG. 7. Variation in relative permittivity of 5 nm BaTiO₃ under different pressure.

reported in the coarse size BTO samples before, and is strong related to the 5 nm unique characters. First, larger surface area of 5 nm BTO will result in a large number of bond defects. These bond defects are in a high energy state and very active. Under certain pressure, the interaction between near by particles will change the disordering state of the Ti off center with respect to the oxygen octahedron,¹⁰ and rebalance the long-range Edward repulsion forces and the short-range hybridized forces, finally leading to a transition. Second, the larger surface and intergrain stresses of smaller nano BTO particles can also change the disordered state.⁹ The stresses will be tuned by external high pressure,^{17,18} as a result leading to a transition around 18 GPa as shown in Fig. 7, which agrees well with the discontinuities in the slopes shown in Fig. 5, indicating structural reordering in the 5 nm BTO particles. The stress results in nonhydrostatic pressure which can broaden the Raman mode in high pressure experiment. The region of 450–630 cm⁻¹ which shows a phase transition as mentioned above at different pressure shift to higher frequency with increasing pressure, while half peak width of this region has no change. So the result of impedance measurements for 5 nm BTO particles show a phase transition appears around 18 GPa.

IV. CONCLUSIONS

In this work, we determined the structural of 5 nm BTO by the combination of the Raman spectrum and the Rietveld refinement using synchrotron X-ray diffraction data. A coexistence of the tetragonal and orthorhombic phases is observed in 5 nm BTO with weight fractions 67(6.6)% and 33(8.0)%, respectively. In the temperature range from -123 °C to 177 °C, the phase boundaries of 5 nm BTO are diffusive and several phases coexist. However, the 5 nm BTO still hold its ferroelectricity in a wide temperature range. The *in-situ* high pressure Raman spectra of 5 nm BTO indicate there are two phase transitions: one is at about 7.5 GPa, which corresponds to the transition to tetragonal phase from the coexisting phases of orthorhombic and tetragonal; the other is around 17.3 GPa, the tetragonal transform to cubic phase, which is further confirmed by the anomaly located at around 18 GPa of the high pressure impedance measurement. After releasing high pressure, the BTO was recovered to the initial state.

ACKNOWLEDGMENTS

This work was supported by the Ministry of Sciences and Technology of China through the 973-Project under Grant Nos. 2009CB623301 and 808204. The authors acknowledge Professor Y. L. Liu and Dr. K. Zhu for their valuable assistance for high pressure Raman scattering experiment. We also acknowledge Dr Y. Li for their valuable assistance for *in situ* impedance measurements, and

Dr. Y. Ren and M. Suchomel for their great help to perform high energy synchrotron diffraction at 11-BM-B, APS, Argonne National Laboratory.

- ¹E. K. Akdogan, M. R. Leonard, and A. Safari, in *Handbook of Low and High Dielectric Constant Materials for Applications*, edited by H. S. Nalwa (Academic, New York, 1999), Vol. 2.
- ²F. Jona and G. Shirane, *Ferroelectric Crystals* (Pergamon Press, London, 1962).
- ³G. A. Samara, *Phys. Rev.* **151**, 378 (1966).
- ⁴D. L. Decker and Y. X. Zhao, *Phys. Rev. B* **39**, 2432 (1989).
- ⁵P. S. Peercy and G. A. Samara, *Phys. Rev. B* **6**, 2748 (1972).
- ⁶M. Fischer and A. Polian, *Phase Transitions* **9**, 205 (1987).
- ⁷A. Jayaraman, J. P. Remeika, and R. S. Katiyar, in *High Pressure in Science and Technology, Proceedings of the 9th AIRAPT International High Pressure Conference. Part 3: General Topics*, Albany, New York, Code 5171 (Mater. Res. Soc. Symp. Proc., 1984), Vol. 22, pp. 165–168. Available at: <http://www.scopus.com/record/display.url?sessionid=B1685134970478FA3008B7D779D411FF.CnvcAmOODVwpVrjSeqQ?eid=2-s2.0-0021627485&origin=inward&txGid=44B393CCCC2FFC35F2AD98A31FAC72AE.WI7NKKC52nnQ.NxjqAQrlA%3a2#>.
- ⁸A. K. Sood, N. Chandrabhas, D. V. S. Muthu, and A. Jayaraman, *Phys. Rev. B* **51**, 8892 (1995).
- ⁹U. D. Venkateswaran, V. M. Naik, and R. Naik, *Phys. Rev. B* **58**, 14256 (1998).
- ¹⁰J. Itié, B. Couzinet, A. Polian, A. Flank, and P. Lagarde, *Europhys. Lett.* **74**, 706 (2006).
- ¹¹B. Ravel, E. Stern, R. Vedrinskii, and V. Kraizman, *Ferroelectrics* **206**, 407 (1998).
- ¹²P. Pruzan, D. Gourdain, J. C. Chervin, B. Canny, B. Couzinet, and M. Hanfland, *Solid State Commun.* **123**, 21 (2002).
- ¹³E. V. Mejía-Uriarte, R. Y. Sato-Berrú, M. Navarrete, M. Villagrán-Muniz, C. Medina-Gutiérrez, C. Frausto-Reyes, and H. Murrietas, *Meas. Sci. Technol.* **17**, 1319 (2006).
- ¹⁴Y. Kobayashi, S. Endo, T. Ashida, L. C. Ming, and T. Kikegawa, *Phys. Rev. B* **61**, 5819 (2000).
- ¹⁵A. Sani, M. Hanfland, and D. Levy, *J. Phys.: Condens. Matter* **14**, 10601 (2002).
- ¹⁶X. H. Wang, X. Y. Deng, W. Hai, and L. T. Li, *Appl. Phys. Lett.* **89**, 162902 (2006).
- ¹⁷J. L. Zhu, C. Q. Jin, W. W. Cao, and X. H. Wang, *Appl. Phys. Lett.* **92**, 242901 (2008).
- ¹⁸S. Lin, T. Q. Lu, C. Q. Jin, and X. H. Wang, *Phys. Rev. B* **74**, 134115 (2006).
- ¹⁹H. Zhang, X. H. Wang, Z. B. Tian, C. F. Zhong, Y. C. Zhang, C. K. Sun, and L. T. Li, *J. Am. Ceram. Soc.* **94**, 3220 (2011).
- ²⁰Y. Wang, Y. H. Han, C. X. Gao, Y. Z. Ma, C. L. Liu, G. Peng, B. J. Wu, B. Liu, T. J. Hu, X. Y. Cui, W. B. Ren, Y. Li, N. N. Su, H. W. Liu, and G. T. Zou, *Rev. Sci. Instrum.* **81**, 013904 (2010).
- ²¹A. C. Larson and R. B. Von Dreele, Los Alamos Natl. Lab., LA (U.S.), LAUR 86–748, 1994.
- ²²J. L. Zhu, W. Han, H. Zhang, Z. Yuan, X. H. Wang, L. T. Li, and C. Q. Jin, *J. Appl. Phys.* **112**, 064110 (2012).
- ²³S. O'Brien, L. Brus, and C. B. Murray, *J. Am. Chem. Soc.* **123**, 12085 (2001).
- ²⁴J. Q. Qi, T. Peng, Y. M. Hu, L. Sun, Y. Wang, W. P. Chen, L. T. Li, C. W. Nan, and H. L. W. Chan, *Nanoscale Res. Lett.* **6**, 466 (2011).
- ²⁵M. Niederberger, N. Pinna, J. Polleux, and M. Antonietti, *Angew. Chem., Int. Ed.* **43**, 2270 (2004).
- ²⁶V. Bansal, P. Poddar, A. Ahmad, and M. Sastry, *J. Am. Chem. Soc.* **128**, 11958 (2006).
- ²⁷R. Y. Sato-Berrú, E. V. Mejía-Uriarte, C. Frausto-Reyes, M. Villagrán-Muniz, H. Murrieta-S, and J. M. Saniger, *Spectrochimica Acta, Part A* **66**, 557 (2007).